# Moments of Superellipsoids and Their Application to Range Image Registration

Aleš Jaklič, *Member, IEEE,* and Franc Solina, *Senior Member, IEEE*

***Abstract*—Cartesian moments are frequently used global geometrical features in computer vision for object pose estimation and recognition. In the paper we derive a closed form expression for 3-D cartesian moment of order $p+q+r$ of a superellipsoid in its canonical coordinate system. We also show how 3-D cartesian moment of a globally deformed superellipsoid in general position and orientation can be computed as a linear combination of 3-D Cartesian moments of the corresponding nondeformed superellipsoid in canonical coordinate system. Additionally, moments of objects that are compositions of superellipsoids can be computed as simple sums of moments of individual parts.**

**To demonstrate practical application of the derived results we register pairs of range images based on moments of recovered compositions of superellipsoids. We use a standard technique to find centers of gravity and principal axes in pairs of range images while third-order moments are used to resolve the four-way ambiguity. Experimental results show expected improvement of recovered rigid transformation based on moments of recovered superellipsoids as compared to the registration based on moments of raw range image data. Besides object pose estimation the presented results can be directly used for object recognition with moments and/or moment invariants as object features.**

***Index Terms*—3-D Cartesian moments, registration, superellipse, superellipsoid, transformations of 3-D moments.**

## I. Introduction

MOMENT-BASED techniques have a well established tradition in object recognition and pose estimation [1]. Initial two-dimensional (2-D) moment invariants techniques were extended to three-dimensions (3-D) [2]–[4], and 3-D moments were used for object-recognition [5].

Although algorithms and methods for segmentation and recovery of superellipsoids exist (see survey in [6]), moment-based methods have not been applied to such representations. Numerical integration was proposed to compute volume and moments of inertia for superellipsoids [7]. However, numerical integration must be performed for each pair of values of shape parameters $\epsilon_1$ and $\epsilon_3$ as well as for each order of moment. Closed-form expressions for computation of moments would thus allow computationally efficient application of moment-based techniques to objects represented as compositions of superellipsoids.

Manuscript received November 11, 2001; revised February 6, 2003. This work was supported by the Ministry of Education, Science and Sports, Republic of Slovenia, Program Computer Vision 1539-506. This paper was recommended by Guest Editor V. Murino.

The authors are with the Computer Vision Laboratory, Faculty of Computer and Information Science, University of Ljubljana, 1001 Ljubljana, Slovenia (e-mail: ales.jaklic@fri.uni-lj.si, franc.solina@fri.uni-lj.si).

Digital Object Identifier 10.1109/TSMCB.2003.814299

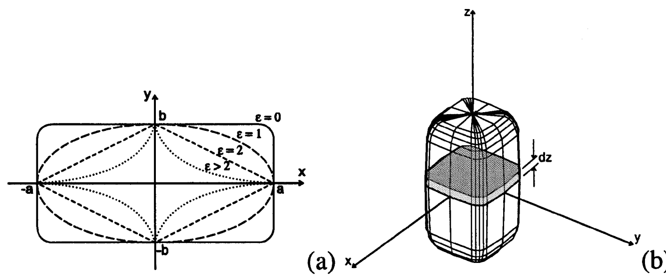


Fig. 1. (a) Superellipses for different values of parameter $\epsilon$. (b) Geometrical interpretation of a superellipsoid as a stack of superellipses with infinitesimal thickness $dz$, their size being modulated by another superellipse.

Recovery of superellipsoids from a single view range image is an under-constrained problem and even additional constraint of minimal volume [8] does not guarantee a precise model for a single superellipsoid like object [9]. In order to obtain a precise model several range images taken from different viewpoints have to be combined into a single data set. Many registration and range data fusion algorithms are based on some form of local minimization and require a good initial estimate of the transformation [10]–[13]. The moment based method presented in this paper could provide such an estimate.

The paper is organized as follows. In Section II, we derive moments of superellipses and based on this result moments of superellipsoids in their respective canonical coordinate systems. Section III presents derivation of transformations of moments of rigidly transformed and/or globally deformed objects. These results are used to compute moments of globally deformed superellipsoids in general position and orientation. Computation of moments of compositions of volumetric parts is addressed in Section IV. Sections V and VI present the registration algorithm based on moments and the experimental results, respectively.

## II. Moments of Superellipses and Superellipsoids

A superellipse is defined as a closed curve in $\mathbb{R}^2$ [see Fig. 1(a)], with parameters $a, b, \epsilon$, and $\omega \in [-\pi, \pi)$

$$\mathbf{r}(\omega) \equiv \begin{bmatrix} x(\omega) \\ y(\omega) \end{bmatrix} \equiv \begin{bmatrix} a(\cos\omega)^{\epsilon} \\ b(\sin\omega)^{\epsilon} \end{bmatrix} \tag{1}$$

while a superellipsoid is defined as a closed surface in $\mathbb{R}^3$ [see Fig. 1(b)], with parameters $a, b, c, \epsilon_1, \epsilon_2$, and $(\eta, \omega) \in [-\pi/2, \pi/2] \times [-\pi, \pi)$ [14]

$$\mathbf{r}(\eta, \omega) \equiv \begin{bmatrix} x(\eta, \omega) \\ y(\eta, \omega) \\ z(\eta, \omega) \end{bmatrix} \equiv \begin{bmatrix} a(\cos\eta)^{\epsilon_1}(\cos\omega)^{\epsilon_2} \\ b(\cos\eta)^{\epsilon_1}(\sin\omega)^{\epsilon_2} \\ c(\sin\eta)^{\epsilon_1} \end{bmatrix}. \tag{2}$$

### A. Two—Dimensional Cartesian Moment of Order $p+q$

The 2-D Cartesian moment $m_{pq}$ of order $p+q$ of a density distribution function $f(x,y)$ is defined as a Riemann integral where $p,q=0,1,2,3,\ldots$

$$m_{pq} \equiv \int_{-\infty}^{+\infty}\int_{-\infty}^{+\infty} x^p y^q f(x,y)\,dx\,dy. \tag{3}$$

Since we are interested in solid moments of a superellipse, we set $f(x,y)=1$ inside the superellipse and $f(x,y)=0$ outside. Due to the symmetry of a superellipse with respect to $x$ and $y$ axis and the origin of the coordinate system, it is easy to note that

$$p \text{ is odd} \vee q \text{ is odd} \Rightarrow m_{pq}=0 \tag{4}$$

while for the case of $p$ and $q$ both being even the moment can be computed using a new coordinate system with coordinates $r$ and $\omega$ instead of $x$ and $y$. The transformation between the two systems is parameterized by $a$, $b$, and $\epsilon$ and given by

$$\begin{aligned} x &= ar(\cos\omega)^\epsilon \\ y &= br(\sin\omega)^\epsilon \end{aligned} \tag{5}$$

with determinant of Jacobian matrix $\mathbf{J}$ for the transformation

$$\det\mathbf{J} = \begin{vmatrix} \frac{\partial x}{\partial r} & \frac{\partial x}{\partial \omega} \\ \frac{\partial y}{\partial r} & \frac{\partial y}{\partial \omega}\end{vmatrix} = abr\epsilon(\sin\omega)^{\epsilon-1}(\cos\omega)^{\epsilon-1}. \tag{6}$$

Since $p$ and $q$ are both even, we can reduce the computation of the integral (3) to the first quadrant of plane $xy$ $(x\geq 0, y\geq 0)$

$$\begin{aligned} m_{pq} &= \int_{-\infty}^{\infty}\int_{-\infty}^{\infty} x^p y^q f(x,y)\,dx\,dy \\ &= 4\int_0^{\infty}\int_0^{\infty} x^p y^q f(x,y)\,dx\,dy \\ &= 4\int_0^{\pi/2}\int_0^1 (ar(\cos\omega)^\epsilon)^p(br(\sin\omega)^\epsilon)^q \det\mathbf{J}\,dr\,d\omega \\ &= \frac{4}{p+q+2}a^{p+1}b^{q+1}\epsilon \\ &\quad\cdot\int_0^{\pi/2}(\sin\omega)^{(q+1)\epsilon-1}(\cos\omega)^{(p+1)\epsilon-1}\,\mathrm{d}\omega \\ &= \frac{2}{p+q+2}a^{p+1}b^{q+1}\epsilon B\left((q+1)\frac{\epsilon}{2},(p+1)\frac{\epsilon}{2}\right) \end{aligned} \tag{7}$$

where the beta function $B(x,y)$ is defined as

$$B(x,y) \equiv 2\int_0^{\pi/2}(\sin\phi)^{2x-1}(\cos\phi)^{2y-1}\,\mathrm{d}\phi. \tag{8}$$

Table I shows the values of the derived expression for some common geometric shapes.

TABLE I
AREAS AND MOMENTS OF INERTIA FOR SUPERELLIPSES OF VARIOUS SHAPES COMPUTED FROM (7) AND USING THE LIMIT (69) FOR CASES WHERE $\epsilon=0$.

| | $\epsilon=0$ (rectangle) | $\epsilon=1$ (ellipse) | $\epsilon=2$ (rhomb) |
|---|---|---|---|
| Area ($m_{00}$) | $4ab$ | $\pi ab$ | $2ab$ |
| Moment of inertia about the $x$ axis ($m_{02}$) | $\frac{4}{3}ab^3$ | $\frac{\pi}{4}ab^3$ | $\frac{1}{3}ab^3$ |
| Moment of inertia about the $y$ axis ($m_{20}$) | $\frac{4}{3}a^3b$ | $\frac{\pi}{4}a^3b$ | $\frac{1}{3}a^3b$ |

### B. Three–Dimensional Cartesian Moments of Order $p+q+r$

The 3-D cartesian moment $m_{pqr}$ of order $p+q+r$ of a density distribution function $f(x,y,z)$ is defined as Riemann integral where $p,q,r=0,1,2,3,\ldots$

$$m_{pqr} \equiv \int_{-\infty}^{+\infty}\int_{-\infty}^{+\infty}\int_{-\infty}^{+\infty} x^p y^q z^r f(x,y,z)\,dx\,dy\,dz. \tag{9}$$

Again we set $f(x,y,z)=1$ inside the superellipsoid and $f(x,y,z)=0$ outside the superellipsoid. The moment can be expressed with a 2-D moment $m_{pq}$ in the plane $z=$ const. parallel to the $xy$ plane as [see Fig. 1(b)]

$$\begin{aligned} m_{pqr} &= \int_{-\infty}^{+\infty} z^r\left(\int_{-\infty}^{+\infty}\int_{-\infty}^{+\infty} x^p y^q f(x,y,z)\,dx\,dy\right)dz \\ &= \int_{-c}^{+c} z^r m_{pq}(z)\,dz. \end{aligned} \tag{10}$$

Intersection of a plane parallel to $xy$ with a superellipsoid is a superellipse with parameters $a(z), b(z)$, and $\epsilon_1$. From (4) and the symmetry of a superellipsoid with respect to the $xy$ plane, it follows that

$$p \text{ is odd} \vee q \text{ is odd} \vee r \text{ is odd} \Rightarrow m_{pqr}=0 \tag{11}$$

and for the case when all of $p,q$, and $r$ are even (with introduction of a new integration variable $\eta$, $z=c(\sin\eta)^{\epsilon_1}$)

$$\begin{aligned} m_{pqr} &= \int_{-c}^{+c} z^r m_{pq}(z)\,dz \\ &= 2\int_0^{\pi/2} z(\eta)^r m_{pq}(\eta)\dot{z}(\eta)\,d\eta \\ &= 2\int_0^{\pi/2}(c(\sin\eta)^{\epsilon_1})^r\left(\frac{2}{p+q+2}a^{p+1}(\eta)b^{q+1}(\eta)\right. \\ &\quad\left.\cdot\,\epsilon_2 B\left((q+1)\frac{\epsilon_2}{2},(p+1)\frac{\epsilon_2}{2}\right)\right)c\epsilon_1(\sin\eta)^{\epsilon_1-1} \\ &\quad\cdot\cos\eta\,\mathrm{d}\eta \\ &= \frac{4}{p+q+2}c^{r+1}\epsilon_1\epsilon_2 B\left((q+1)\frac{\epsilon_2}{2},(p+1)\frac{\epsilon_2}{2}\right) \\ &\quad\cdot\int_0^{\pi/2}(\sin\eta)^{\epsilon_1(r+1)-1}(a(\cos\eta)^{\epsilon_1})^{p+1} \\ &\quad\times(b(\cos\eta)^{\epsilon_1})^{q+1}\cdot\cos\eta\,\mathrm{d}\eta \\ &= \frac{4}{p+q+2}a^{p+1}b^{q+1}c^{r+1}\epsilon_1\epsilon_2 \\ &\quad\cdot B\left((q+1)\frac{\epsilon_2}{2},(p+1)\frac{\epsilon_2}{2}\right) \\ &\quad\cdot\int_0^{\pi/2}(\sin\eta)^{\epsilon_1(r+1)-1}(\cos\eta)^{\epsilon_1(p+q+2)+1}\,\mathrm{d}\eta \\ &= \frac{2}{p+q+2}a^{p+1}b^{q+1}c^{r+1}\epsilon_1\epsilon_2 \\ &\quad\cdot B\left((r+1)\frac{\epsilon_1}{2},(p+q+2)\frac{\epsilon_1}{2}+1\right) \\ &\quad\cdot B\left((q+1)\frac{\epsilon_2}{2},(p+1)\frac{\epsilon_2}{2}\right). \end{aligned} \tag{12}$$

Moments of common geometric shapes computed from (12) are presented in Table II. They correspond exactly to the well-

TABLE II
VOLUMES AND MOMENTS OF INERTIA FOR SUPERELLIPSOIDS OF VARIOUS SHAPES COMPUTED FROM (12) AND USING LIMITS (69), (70) FOR CASES WHERE $\epsilon_1 = 0$ OR $\epsilon_2 = 0$.

| | $\epsilon_1 = 0$, $\epsilon_2 = 0$ (plate) | $\epsilon_1 = 0$, $\epsilon_2 = 1$ (elliptical cylinder) | $\epsilon_1 = 1$, $\epsilon_1 = 1$ (ellipsoid) |
|---|---|---|---|
| $V$ | $8abc$ | $2\pi abc$ | $\frac{4}{3}\pi abc$ |
| $I_{xx}$ | $\frac{8}{3}abc(b^2 + c^2)$ | $\pi abc(\frac{1}{2}b^2 + \frac{2}{3}c^2)$ | $\frac{4}{15}\pi abc(b^2 + c^2)$ |
| $I_{yy}$ | $\frac{8}{3}abc(a^2 + c^2)$ | $\pi abc(\frac{1}{2}a^2 + \frac{2}{3}c^2)$ | $\frac{4}{15}\pi abc(a^2 + c^2)$ |
| $I_{zz}$ | $\frac{8}{3}abc(a^2 + b^2)$ | $\pi abc(\frac{1}{2}a^2 + \frac{1}{2}b^2)$ | $\frac{4}{15}\pi abc(a^2 + b^2)$ |

known expressions derived by direct integration for those specific shapes [4].

## III. TRANSFORMATIONS OF MOMENTS

Practical applications of superellipsoid models require their expression in arbitrary position and orientation in space as well as enhancement of their shape modeling capabilities with global deformations [6], [8], [15]. Both types of enhancements can be represented as a mapping from points of an object in coordinate system $x, y, z$ to points of a transformed objects in a new coordinate system $X, Y, Z$

$$\begin{aligned} X &= f_x(x, y, z) \\ Y &= f_y(x, y, z) \\ Z &= f_z(x, y, z). \end{aligned} \tag{13}$$

To compute moments $M_{pqr}$ of a transformed object in coordinate system $X, Y, Z$ integration has to be performed over the volume $(V)$ bounded by the mapping of original volume $(v)$. This can be changed to integration over the volume $(v)$ bounded by original object by a change of variables in the multiple integral and using the determinant of Jacobian matrix of the mapping

$$\det \mathbf{J} = \det \begin{bmatrix} \frac{\partial X}{\partial x}, & \frac{\partial X}{\partial y} & \frac{\partial X}{\partial z} \\ \frac{\partial Y}{\partial x}, & \frac{\partial Y}{\partial y} & \frac{\partial Y}{\partial z} \\ \frac{\partial Z}{\partial x}, & \frac{\partial Z}{\partial y} & \frac{\partial Z}{\partial z} \end{bmatrix}. \tag{14}$$

The corresponding moments in the coordinate system $X, Y, Z$ and in the coordinate system $x, y, z$ are denoted as $M_{pqr}$ and $m_{pqr}$, respectively

$$\begin{aligned} M_{pqr} &= \iiint_V X^p Y^q Z^r \, dX \, dY \, dZ \\ &= \iiint_v f_x(x, y, z)^p f_y(x, y, z)^q f_z(x, y, z)^r \\ &\quad \cdot \det \mathbf{J} \, dx \, dy \, dz. \end{aligned} \tag{15}$$

If functions $f_x, f_y, f_z$ are polynomials with multiple variables $x, y, z$, the determinant of Jacobian matrix is also a polynomial of the same kind and the whole integrand in (15) can be expanded as a linear combination of moments of the original object. Alternatively, nonpolynomial functions $f_x, f_y, f_z$ can be approximated with polynomial functions using a Taylor expansion. In the following subsections we present detailed results for translation, rotation, linear tapering and parabolic bending. Appendix B presents a program in Mathematica that can assist in derivations of expressions for a particular moment. Note that the derived results are applicable to any shape not just superellipsoids.

### A. Object Translation

Translation is defined by a mapping

$$\begin{aligned} f_x(x, y, z) &= x + p_x \\ f_y(x, y, z) &= y + p_y \\ f_z(x, y, z) &= z + p_z \end{aligned} \tag{16}$$

where

$$\det \mathbf{J} = \det \begin{bmatrix} 1, & 0 & 0 \\ 0, & 1 & 0 \\ 0, & 0 & 1 \end{bmatrix} = 1 \tag{17}$$

and by using binomial theorem, it follows that

$$\begin{aligned} M_{pqr} &= \iiint_v (x + p_x)^p (y + p_y)^q (z + p_z)^r \, dx \, dy \, dz \\ &= \sum_{i=0}^{p} \sum_{j=0}^{q} \sum_{k=0}^{r} \binom{p}{i} \binom{q}{j} \binom{r}{k} p_x^{p-i} p_y^{q-j} p_z^{r-k} m_{ijk}. \end{aligned} \tag{18}$$

Moment $M_{pqr}$ of order $n$ of a translated object is thus a linear combination of moments $m_{pqr}$ of order less or equal to $n$ of the original object.

### B. Object Rotation

Rotation is defined by a mapping

$$\begin{aligned} f_x(x, y, z) &= n_x x + o_x y + a_x z \\ f_y(x, y, z) &= n_y x + o_y y + a_y z \\ f_z(x, y, z) &= n_z x + o_z y + a_z z \end{aligned} \tag{19}$$

where the Jacobian matrix is equal to an orthonormal rotation matrix

$$\det\mathbf{J} = \det \begin{bmatrix} n_x, & o_x & a_x \\ n_y, & o_y & a_y \\ n_z, & o_z & a_z \end{bmatrix} = 1 \tag{20}$$

and with the use of the multinomial theorem to expand the power terms we derive

$$\begin{aligned} M_{pqr} &= \iiint_v (n_x x + o_x y + a_x z)^p (n_y x + o_y y + a_y z)^q \\ &\quad \cdot (n_z x + o_z y + a_z z)^r \, dx \, dy \, dz \\ &= \sum_{\substack{i+j+k \\ =p}} \sum_{\substack{l+m+n \\ =q}} \sum_{\substack{t+u+v \\ =r}} (i, j, k)!(l, m, n)!(t, u, v)! \\ &\quad \cdot n_x^i o_x^j a_x^k n_y^l o_y^m a_y^n n_z^t o_z^u a_z^v \\ &\quad \cdot m_{(i+l+t)(j+m+u)(k+n+v)}. \end{aligned} \tag{21}$$

Note that moment $M_{pqr}$ of order $n$ of a rotated object is a linear combination of moments $m_{pqr}$ of the same order $n$ of the original object.

### C. Rigid Object Transformation—Rotation and Translation

Any rigid transformation can be decomposed into rotation followed by translation and described by

$$\begin{aligned} f_x(x,y,z) &= n_x x + o_x y + a_x z + p_x \\ f_y(x,y,z) &= n_y x + o_y y + a_y z + p_y \\ f_z(x,y,z) &= n_z x + o_z y + a_z z + p_z \end{aligned} \tag{22}$$

where

$$\det \mathbf{J} = \det \begin{bmatrix} n_x, & o_x & a_x \\ n_y, & o_y & a_y \\ n_z, & o_z & a_z \end{bmatrix} = 1. \tag{23}$$

A general expression for $M_{pqr}$ can be derived analogously to (21) using multinomial theorem.

$$\begin{aligned} M_{pqr} = & \sum_{\substack{i+j+k+l \\ =p}} \sum_{\substack{m+n+o+s \\ =q}} \sum_{\substack{t+u+v+w \\ =r}} (i,j,k,l)!(m,n,o,s)! \\ & \cdot (t,u,v,w)! n_x^i o_x^j a_x^k p_x^l n_y^m o_y^n a_y^o p_y^s n_z^t o_z^u a_z^v p_z^w \\ & \cdot m_{(i+m+t)(j+n+u)(k+o+v)} \end{aligned} \tag{24}$$

where multinomial coeficients are defined as

$$(n_1, n_2, \ldots, n_k)! = \frac{(n_1 + n_2 + \cdots + n_k)!}{n_1! n_2! \cdots n_k!}. \tag{25}$$

However, as order of moment increases, the number of terms in polynomial expansion increases very rapidly in case of a general object. In those cases it is easier to decompose the rigid transformation into rotation followed by translation and apply two separate transformations in a sequence to the original moments. Symmetry of superellipsoids further simplifies the computation of expressions since most moments are equal to 0 in the canonical coordinate system.

### D. Linear Tapering

Linear tapering along the $z$ axis is defined as [8]

$$\begin{aligned} f_x(x,y,z) &= \left(\frac{k_x}{c} z + 1\right) x \quad -1 \le k_x \le 1 \\ f_y(x,y,z) &= \left(\frac{k_y}{c} z + 1\right) y \quad -1 \le k_y \le 1 \\ f_z(x,y,z) &= z \end{aligned} \tag{26}$$

with

$$\begin{aligned} \det \mathbf{J} &= \det \begin{bmatrix} \frac{k_x}{c} z + 1 & 0 & \frac{k_x}{c} x \\ 0 & \frac{k_y}{c} z + 1 & \frac{k_y}{c} y \\ 0 & 0 & 1 \end{bmatrix} \\ &= \left(\frac{k_x}{c} z + 1\right)\left(\frac{k_y}{c} z + 1\right) \end{aligned} \tag{27}$$

and allows for modeling of cones and pyramids with superellipsoids. The mapping parameters $k_x$ and $k_y$ are constrained to prevent a degenerate transformation for the case of superellipsoids. Moments of a tapered superellipsoid are related to moments of a nondeformed superellipsoid as follows

$$\begin{aligned} M_{pqr} &= \iiint_v \left(\frac{k_x}{c} z + 1\right)^p x^p \left(\frac{k_y}{c} z + 1\right)^q \\ &\quad \cdot y^q z^r \left(\frac{k_x}{c} z + 1\right) \cdot \left(\frac{k_y}{c} z + 1\right) dx\, dy\, dz \\ &= \iiint_v \left(\frac{k_x}{c} z + 1\right)^{p+1} \left(\frac{k_y}{c} z + 1\right)^{q+1} \\ &\quad \cdot x^p y^q z^r \, dx\, dy\, dz \\ &= \sum_{i=0}^{p+1} \sum_{j=0}^{q+1} \binom{p+1}{i} \binom{q+1}{j} \frac{k_x^i k_y^j}{c^{i+j}} \\ &\quad \cdot \iiint_v x^p y^q z^{r+i+j} \, dx\, dy\, dz \\ &= \sum_{i=0}^{p+1} \sum_{j=0}^{q+1} \binom{p+1}{i} \binom{q+1}{j} \frac{k_x^i k_y^j}{c^{i+j}} m_{pq(r+i+j)}. \end{aligned} \tag{28}$$

For illustration we use (28) to derive volume $V$, center of gravity $(c_x, c_y, c_z)$, and moment of inertia about the $z$ axis of a right circular cone from the moments $m_{pqr}$ of a nondeformed superellipsoid. A circular cone with radius $r$ and height $h$ can be modeled as a tapered superellipsoid, with the following parameters $a = b = r/2, c = h/2, \epsilon_1 = 0, \epsilon_2 = 1$ and $k_x = -1, k_y = -1$.

$$V = M_{000} = m_{000} + \frac{k_x k_y}{c^2} m_{002} = \frac{\pi}{3} r^2 h \tag{29}$$

$$c_x = \frac{M_{100}}{M_{000}} = 0 \tag{30}$$

$$c_y = \frac{M_{010}}{M_{000}} = 0 \tag{31}$$

$$c_z = \frac{M_{001}}{M_{000}} = \frac{\frac{k_x + k_y}{c} m_{002}}{m_{000} + \frac{k_x k_y}{c^2} m_{002}} = -\frac{h}{4} \tag{32}$$

$$\begin{aligned} I_{zz} = M_{200} + M_{200} &= m_{020} + \left(\frac{3k_x k_y}{c^2} + \frac{3k_y^2}{c^2}\right) m_{022} \\ &+ \frac{k_x k_y^3}{c^4} m_{024} + m_{200} + \left(\frac{3k_x k_y}{c^2} + \frac{3k_x^2}{c^2}\right) m_{202} \\ &+ \frac{k_x^3 k_y}{c^4} m_{204} = \frac{\pi}{10} r^4 h \end{aligned} \tag{33}$$

### E. Parabolic Bending

Circular bending introduced in [8] and [15] cannot be represented as a mapping with polynomial functions. However, for slight bending, it can be approximated by parabolic bending. A cross-section parallel to plane $xy$ of an object is translated in the direction of a unit vector $(\cos\alpha, \sin\alpha)$ with orientation angle $\alpha$ and magnitude proportional with $s$ to $z^2$

$$\begin{aligned} f_x(x,y,z) &= x + s \ \cos\, \alpha\, z^2 \\ f_y(x,y,z) &= y + s \ \sin\, \alpha\, z^2 \\ f_z(x,y,z) &= z \end{aligned} \tag{34}$$

where

$$\det \mathbf{J} = \det \begin{bmatrix} 1, & 0 & 2s\cos\alpha \mathrm{z} \\ 0, & 1 & 2s\sin\alpha \mathrm{z} \\ 0, & 0 & 1 \end{bmatrix} = 1 \tag{35}$$

and

$$\begin{aligned} M_{pqr} &= \iiint_v (x + s\cos\alpha z^2)^p \\ &\quad \cdot (y + s\sin\alpha z^2)^q z^r \, dx\, dy\, dz \\ &= \sum_{i=0}^{p}\sum_{j=0}^{q} \binom{p}{i}\binom{q}{j} s^{p+q-i-j} \cos^{\mathrm{p-i}}\alpha \sin^{\mathrm{q-j}}\alpha \\ &\quad \cdot \iiint_v x^i y^j z^{r+2(p+q-i-j)} \, dx\, dy\, dz \\ &= \sum_{i=0}^{p}\sum_{j=0}^{q} \binom{p}{i}\binom{q}{j} s^{p+q-i-j} \cos^{p-i}\alpha \sin^{q-j}\alpha \\ &\quad \cdot m_{ij(r+2(p+q-i-j))}. \end{aligned} \tag{36}$$

### F. Compositions of Transformations

Transformations can be combined into sequences of transformations. For the case of recovering superellipsoids, the following sequence is usually used [8], [15]

$$\text{Translate}\left(\text{Rotate}(\text{Bend}(\text{Taper}(\mathbf{x})))\right). \tag{37}$$

In order to compute moments of such transformed shape primitives, moments of superellipsoids have to be transformed in the same sequence order.

## IV. Moments of Compositions of Volumetric Parts

Objects can be modeled with individual volumetric parts that are glued together, or, as a union of their volumes which allows for penetration of parts into each other. We will discus a case of two penetrating volumetric parts $V_1$ and $V_2$ with density distribution functions $f_1(x,y,z)$ and $f_2(x,y,z)$ equal to 1 within the volumes of $V_1$ and $V_2$ and equal to 0 outside. We assume that in region $V_1 \cap V_2$ the density distribution function $f(x,y,z)$ is the sum of $f_1$ and $f_2$. In other words, the value of the density function $f(x,y,z)$ is equal to the number of volumetric parts that include point $(x,y,z)$. The moment of such a composition is a sum of moments of individual parts

$$\begin{aligned} m_{pqr} &= \iiint_{V_1\cup V_2} x^p y^q z^r \\ &\quad \cdot (f_1(x,y,z) + f_2(x,y,z))\, dx\, dy\, dz \\ &= \iiint_{V_1\setminus(V_1\cap V_2)} x^p y^q z^r f_1(x,y,z)\, dx\, dy\, dz \\ &\quad + \iiint_{V_2\setminus(V_1\cap V_2)} x^p y^q z^r f_2(x,y,z)\, dx\, dy\, dz \\ &\quad + \iiint_{V_1\cap V_2} x^p y^q z^r f_1(x,y,z)\, dx\, dy\, dz \\ &\quad + \iiint_{V_1\cap V_2} x^p y^q z^r f_2(x,y,z)\, dx\, dy\, dz \\ &= \iiint_{V_1} x^p y^q z^r f_1(x,y,z)\, dx\, dy\, dz \\ &\quad + \iiint_{V_2} x^p y^q z^r f_2(x,y,z)\, dx\, dy\, dz \\ &= m_{pqr}^{V_1} + m_{pqr}^{V_2}. \end{aligned} \tag{38}$$

The result can be generalized to an arbitrary number of parts by a simple induction.

## V. Range Image Registration

The basic idea of range image registration based on moments is to construct a coordinate frame which is rigidly attached to the object in each image [1], [3], [5]. After constructing the two frames, we know their relationship to the global coordinate system and thus we also know the rigid transformation between the two frames, which is also the rigid transformation of the object. We will name the constructed frames the canonical frames. The canonical frame is constructed in two steps as follows [5]

1) In the first step, the global coordinate system $G$ is translated to the center of gravity of the object $(c_x, c_y, c_z)$ to form coordinate system $C'$. Moments of individual superellipsoid parts $(m_{pqr}^i)$ are transformed to the global coordinate system $(M_{pqr}^i)$ and summed over the number of parts $N$ to compute the center of gravity.

$$V = \sum_{i=1}^{N} M_{000}^i \tag{39}$$

$$c_x = \frac{1}{V}\sum_{i=1}^{N} M_{100}^i \tag{40}$$

$$c_y = \frac{1}{V}\sum_{i=1}^{N} M_{010}^i \tag{41}$$

$$c_z = \frac{1}{V}\sum_{i=1}^{N} M_{001}^i \tag{42}$$

First-order moments of the object computed in $C'$ are equal to 0.

2) In the second step, the axes of coordinate system $C'$ from the first step are rotated so that the axes are aligned along the axes of minimal and maximal moment of inertia. This rotation produces coordinate system $C''$, and the inertia matrix $\mathbf{I}''$ computed in frame $C''$ is diagonal. The direction of the axes of $C''$ correspond to the eigenvectors of the inertia matrix

$$\mathbf{I}' = \begin{bmatrix} I'_{xx} & -I'_{xy} & -I'_{xz} \\ -I'_{yx} & I'_{yy} & -I'_{yz} \\ -I'_{zx} & -I'_{zy} & I'_{zz} \end{bmatrix} \tag{43}$$

$$I'_{xx} = \sum_{i=1}^{N}\left(M'^i_{020} + M'^i_{002}\right) \tag{44}$$

$$I'_{yy} = \sum_{i=1}^{N}\left(M'^i_{200} + M'^i_{002}\right) \tag{45}$$

$$I'_{zz} = \sum_{i=1}^{N}\left(M'^i_{200} + M'^i_{020}\right) \tag{46}$$

$$I'_{xy} = \sum_{i=1}^{N} M'^i_{110} \tag{47}$$

$$I'_{xz} = \sum_{i=1}^{N} M'^i_{101} \tag{48}$$

$$I'_{yz} = \sum_{i=1}^{N} M'^i_{011} \tag{49}$$

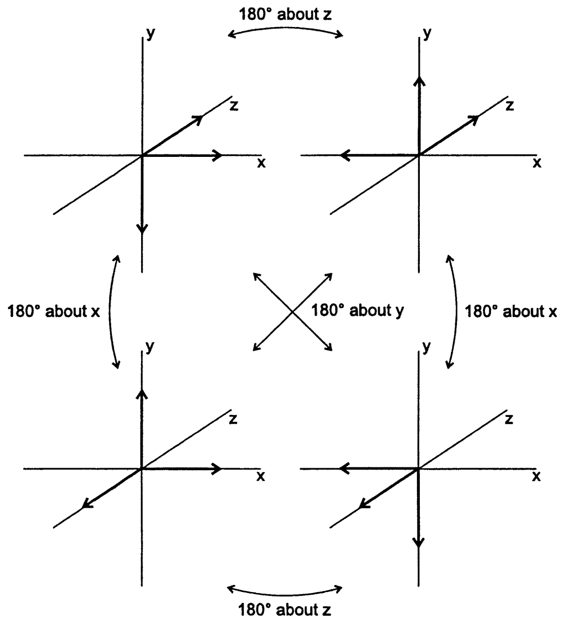


Fig. 2. Four different right-hand Cartesian coordinate frames with their axes aligned along given lines. Each one of them generates the remaining three by rotations of 180° about all the axes.

where moments ${M'}^{i}_{pqr}$ are computed in the $C'$. For our work we freely selected the $x$ and the $z$ axes of $C''$ to correspond to the minimal and to the maximal moment of inertia, respectively. Since we are dealing only with right-hand Cartesian coordinate frames, we uniquely determine the remaining third axis by fixing any two axes of the coordinate system.

Note, however, that the moments of inertia are invariant to rotation of the coordinate frame for 180° about any of the coordinate axes or in other words, if $\mathbf{u}$ is an eigenvector of $\mathbf{I}'$ so is the $-\mathbf{u}$. This leads to four possible orientations of the canonical coordinate frame $C''$ depicted in Fig. 2 [5]. How does this four-way ambiguity influence image registration? In the first view we can clearly freely select one of the frames $C''$. This frame is uniquely related to spatial distribution of the object, unless the object is symmetrical. In the second view we now have four candidate frames and only one is related to the object in the second view in the same spatial way as the chosen frame in the first view. The problem is how to find this frame or the correct transformation. It is illustrated in Fig. 3.

### A. Resolving Four-Way Ambiguity

A search for the most distant point on the object from the origin of the coordinate system along the principal axes was proposed in [5], and the use of third order moments in [3], to resolve the four-way ambiguity. The presented approach is similar to [3], but with much simpler derivation.

It is instructive to determine how solid moments of the same object computed in the four coordinate frames are related. Let $M_{pqr}$ be a moment of an object computed in a Cartesian coordinate system, then it is easy to show that moments of the same object in the coordinate systems that are rotated for 180° about $x, y$, and $z$ axes, respectively, are related as follows:

$$M^x_{pqr} = (-1)^{q+r} M_{pqr} \tag{50}$$

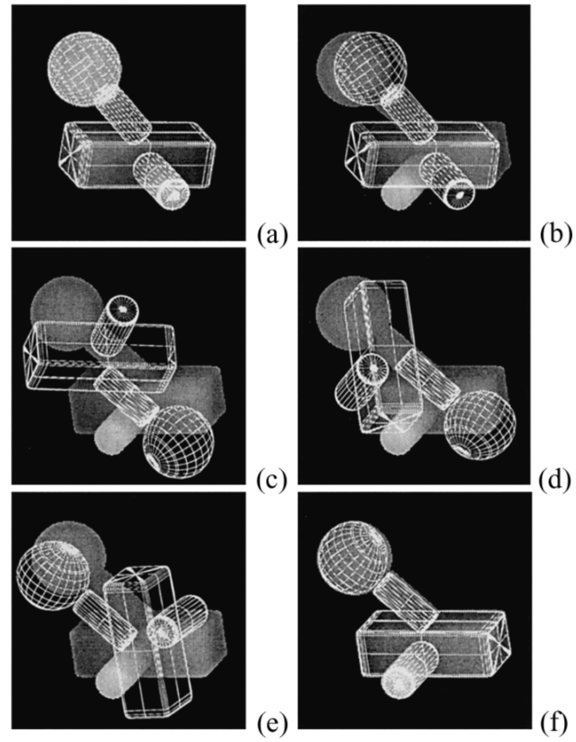


Fig. 3. Registration based on moments produces four possible solutions for the canonical frame $C''$. (a) View-1 range image and recovered model-1 (b) view-2 range image with overlaid model-1 using unit transformation $\mathbf{T} = \mathbf{I}$, (c)–(f) represent view-2 range image overlaid with model-1 transformed with four possible transformations. Only the transformation depicted in (f) is correct.

$$M^y_{pqr} = (-1)^{p+r} M_{pqr} \tag{51}$$

$$M^z_{pqr} = (-1)^{p+q} M_{pqr}. \tag{52}$$

We can now answer the question if moments can be used as features to resolve the four-way ambiguity. The zeroth-order moment cannot be used since it is invariant to any rigid transformation. Similarly, all first-order moments computed in frames $C''$ are 0 by definition of $C''$. Second-order moments $m_{110}, m_{011}, m_{101}$ are equal to 0 in frame $C''$ by definition, while $m_{200}, m_{020}, m_{002}$ are invariant to rotations that generate frames $C''$. Only third and higher order moments computed in frames $C''$ provide sufficient information to distinguish frames $C''$.

We propose the following algorithm to resolve the four-way ambiguity

1) We select any frame from the first view and compute a vector of moments in selected frame

$$\mathbf{v} = (m_{300}, m_{210}, m_{201}, m_{120}, m_{111} \\ m_{102}, m_{030}, m_{021}, m_{012}, m_{003}). \tag{53}$$

2) We select any frame from the second view and compute a vector of moments in selected frame

$$\mathbf{v}' = \mathbf{v}'_0 = (m'_{300}, m'_{210}, m'_{201}, m'_{120}, m'_{111} \\ m'_{102}, m'_{030}, m'_{021}, m'_{012}, m'_{003}) \tag{54}$$

and the remaining 3 from $\mathbf{v}'$

$$\mathbf{v}'_\mathbf{x} = \mathbf{v}'_1 = (m'_{300}, -m'_{210}, -m'_{201}, m'_{120}, m'_{111} \\ m'_{102}, -m'_{030}, -m'_{021}, -m'_{012}, -m'_{003}) \tag{55}$$

$$\mathbf{v}'_\mathbf{y} = \mathbf{v}'_2 = (-m'_{300}, m'_{210}, -m'_{201}, -m'_{120}, m'_{111}$$

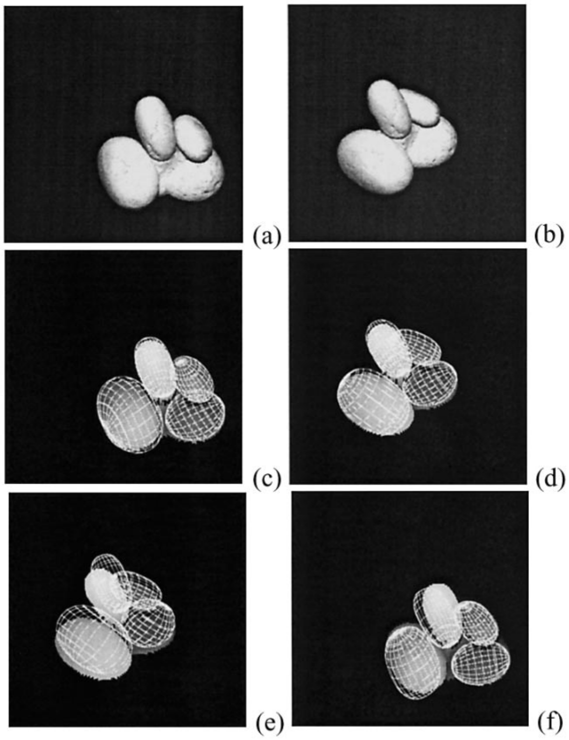

Fig. 4. Registration of two real range images based on recovered superellipsoids. (a) Intensity image view1. (b) Intensity image view2. (c) Range image view1 with recovered superellipsoids. (d) Range image2 with recovered superellipsoids. (e) Models recovered from view2 overlaid over range image view1 using the recovered transformation. (f) Models recovered from view1 overlaid over range image2 using the recovered transformation. Residual transformation: $\mathbf{t} = (18.21, 21.84, -5.91), \mathbf{n} = (-0.72, -0.62, -0.69), \theta = 9.6°$.

$$-m'_{102}, m'_{030}, -m'_{021}, m'_{012}, -m'_{003}) \tag{56}$$

$$\mathbf{v}'_{\mathbf{z}} = \mathbf{v}'_3 = (-m'_{300}, -m'_{210}, m'_{201}, -m'_{120}, m'_{111} \\ -m'_{102}, -m'_{030}, m'_{021}, -m'_{012}, m'_{003}). \tag{57}$$

3) The corresponding frame $i$ in the second view is the one with vector that minimizes

$$\|\mathbf{v} - \mathbf{v}'_i\|. \tag{58}$$

Note that if third-order moments are equal to 0 due to object shape or the vector $\mathbf{v}$ is equidistant to several vectors, higher order moments may be used in the same way.

## VI. Experimental Results

In the first experiment (Fig. 4) we recovered estimate of a rigid transformation between two range image views of a pile of stones. Algorithm described in [6] and [16] was used to recover superellipsoid models from range images. The ground truth transformation $\mathbf{T}_{\text{true}}$ was computed from seven pairs of range points corresponding to small dents visible in the grayscale images of both views. The pairs of features were manually selected. We used a least-square method described in [17] to compute $\mathbf{T}_{\text{true}}$. The estimate of transformation $\mathbf{T}_{\text{estimate}}$ was then computed based on moments of recovered superellipsoids in each view, and the residual transformation $\mathbf{T}_{\text{residual}}$ was computed from (59). All transformations were represented with homogeneous transformation matrices.

$$\mathbf{T}_{\text{true}} = \mathbf{T}_{\text{residual}}\mathbf{T}_{\text{estimate}}. \tag{59}$$

A precise $\mathbf{T}_{\text{estimate}}$ would yield $\mathbf{T}_{\text{residual}}$ equal to an identity matrix. The residual transformation was decomposed into rotation followed by translation $(\mathbf{t})$. The rotation was represented by a unit vector in direction of axis of rotation $(\mathbf{n})$ and an angle of rotation $(\theta)$. To visualize the quality of recovered estimate of the rigid transformation we overlaid the recovered models from view2 over the range image view1 [Fig. 4(e)] and recovered models from view1 over the range image view2 [Fig. 4(f)].

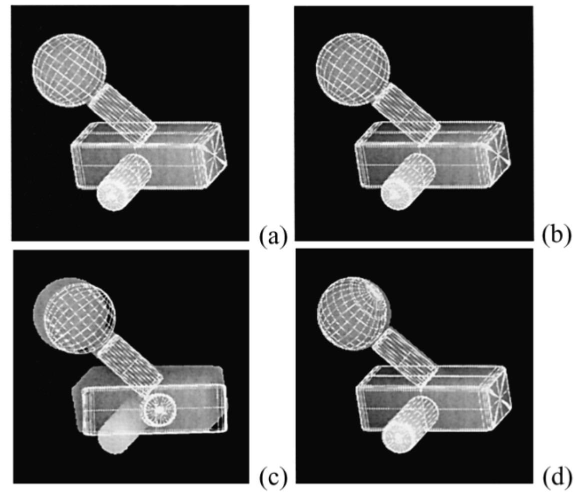

Fig. 5. Comparison of recovered rigid transformations based on moments of recovered models to recovered rigid transformation based on moments of range data points. (a) First view. (b) Second view. (c) Recovered rigid transformations based on moments of range data, residual transformation $\mathbf{t} = (68.21, 71.84, -75.91), \mathbf{n} = (-0.67, -0.74, -0.08), \theta = 33.6°$ (d) recovered rigid transformations based on moments of recovered models, residual transformation $\mathbf{t} = (0.83, -0.74, -2.17), \mathbf{n} = (-0.19, -0.90, 0.38), \theta = 0.9°$.

In the second experiment (Figs. 5–7), we generated a set of synthetic range images of an object modeled with superellipsoids to exclude errors due to nonsuperellipsoid shapes in object domain. Estimates of rigid transformations were computed based on *moments of recovered superellipsoids* and another set of estimates based on *moments of range image data points* where moments of the objects were approximated as sums over $N$ range data points $(x_i, y_i, z_i)$

$$m_{pqr} = \sum_{i=1}^{N} x_i^p y_i^q z_i^r. \tag{60}$$

Ground truth transformations used in generation of synthetic range images were used to compute residual transformations. The results presented in Figs. 5–7 compare precision of estimates computed from moments of recovered models to estimates based on moments of range image data points. Figures marked with (a) and (b) represent range images overlaid with wire frames of recovered superellipsoids of the first and the second view respectively. Figs. (c) represent range image of the second view overlaid by the recovered model from the first view using transformation estimate computed from *moments of raw range image data points* from (60). Similarly, Figs. (d) show range image of the second view overlaid by the recovered

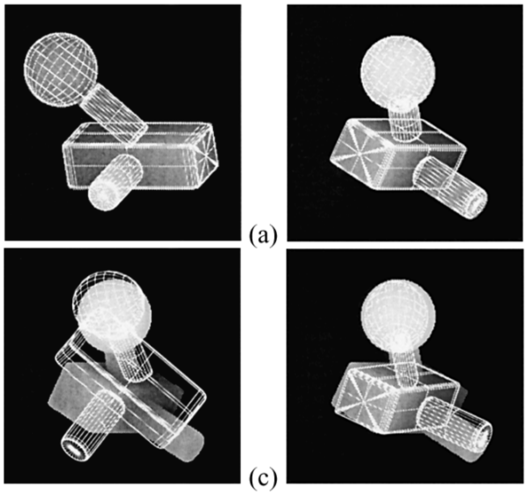

(a) (b) (c) (d)

Fig. 6. Comparison of recovered rigid transformations based on moments of recovered models to recovered rigid transformation based on moments of range data points. (a) First view. (b) Second view. (c) Recovered rigid transformations based on moments of range data, residual transformation $\mathbf{t} = (101.1, -121.1, 120.1), \mathbf{n} = (-0.12, 0.74, 0.65), \theta = 81.6°$, (d) recovered rigid transformations based on moments of recovered models, residual transformation $\mathbf{t} = (0.1, 16.7, -10.4), \mathbf{n} = (-0.02, 0.51, 0.86), \theta = 8.4°$.

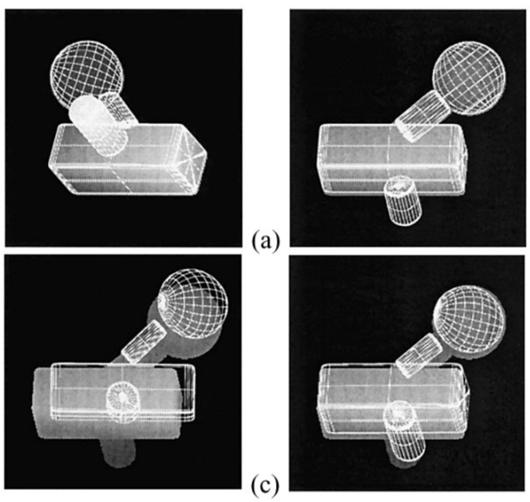

(a) (b) (c) (d)

Fig. 7. Comparison of recovered rigid transformations based on moments of recovered models to recovered rigid transformation based on moments of range data points. (a) First view. (b) Second view. (c) Recovered rigid transformations based on moments of range data, residual transformation $\mathbf{t} = (1.4, -68.1, -3.5), \mathbf{n} = (0.94, 0.33, 0.04), \theta = 21.6°$, (d) recovered rigid transformations based on moments of recovered models, residual transformation $\mathbf{t} = (0.1, 16.7, -10.4), \mathbf{n} = (0.52, -0.81, 0.28), \theta = 1.4°$.

model from the first view using transformation estimate computed from *moments of recovered superellipsoid models*. Comparison of parameters of residual transformations clearly shows that the method based on moments of recovered superellipsoid models is superior to the method based on moments of raw range image data points. On the other hand, the estimate based on moments of recovered superellipsoids is not completely precise since it is not possible to recover a precise superellipsoid model from a single range image.

The error residuals of recovered estimates in case of real and synthetic range images were less than 10° in rotation and less than 10% of the object size in translation.

## VII. Conclusion

We derived closed-form expressions for 2–D Cartesian moment $m_{pq}$ of order $p+q$ of a superellipse and the 3–D Cartesian moment $m_{pqr}$ of order $p+q+r$ of a superellipsoid. These results can be directly used to compute zeroth, first, and second-order moments with well-known physical meaning as area or volume, center of gravity and moments of inertia as well as to compute higher order moments used in applications of various moment invariants. To demonstrate the correctness of derived expressions, we computed area and moments of inertia for standard 2–D shapes (rectangle, ellipse, rhomb) and volume and moments of inertia for standard 3–D shapes (plate, elliptical cylinder, ellipsoid). We further showed how moments of a transformed object can be computed as linear combinations of moments of the original object if the transformation can be represented with polynomials. Explicit derivations were given for translation, rotation, linear tapering and parabolic bending as well as their combinations.

Feasibility of the proposed registration method based on moments was demonstrated with a registration of two real range views. Experiments with synthetic range images and know ground truth transformation showed significantly better performance of range image registration based on moments of recovered superellipsoid models as compared to registration based on moments of range image data points. This is due to reduced effects of self-occlusion of parts and independence of computed moments on the density of range image data points. The error residuals of recovered estimates were less than 10° in rotation and less than 10% of the object size in translation.

The presented results can also be used for object recognition with moments and/or moment invariants as object features.

## Appendix I
## Beta and Gamma Functions

Beta function is defined as

$$B(x,y) \equiv 2\int_0^{\pi/2} (\sin\phi)^{2x-1}(\cos\phi)^{2y-1}\, d\phi \tag{61}$$

and related to gamma function as follows

$$B(x,y) = \frac{\Gamma(x)\Gamma(y)}{\Gamma(x+y)}. \tag{62}$$

For completeness we provide the definition of the gamma function

$$\Gamma(x) = \int_0^{+\infty} t^x e^{-t}\, dt \tag{63}$$

and the well know equalities for the gamma function used in further derivations

$$\Gamma(x+1) = x\Gamma(x) \tag{64}$$

$$\Gamma(n) = (n-1)! \tag{65}$$

$$\Gamma(1/2) = \sqrt{\pi}. \tag{66}$$

```
fx = (kx/c z  + 1)x
fy = (ky/c z + 1) y
fz = z
J = {{D[fx, x] , D[fy, x], D[fz, x]},
     {D[fx, y] , D[fy, y], D[fz, y]},
     {D[fx, z] , D[fy, z], D[fz, z]}}
integrand[p_, q_, r_] := fx^p fy^q fz^r Det[J]
(* begin - remove this section if *)
(* the object tran. is not a superellipsoid *)
 M[p_Integer, q_Integer, r_Integer]  :=
    If[OddQ[p] || OddQ[q] || OddQ[r],
                                 0, msq[p, q, r]]
(* end - remove this section if *)
(* the object tran. is not a superellipsoid *)
Mdef[p_, q_, r_] :=
  Apply[Plus,
   Flatten[CoefficientList[integrand[p, q, r],
     {x, y, z}] ] *
     Flatten[Table[
     M[i, j, k],
     {i, 0, Exponent[integrand[p, q, r], x]},
     {j, 0, Exponent[integrand[p, q, r], y]},
     {k, 0, Exponent[integrand[p, q, r], z]}
]]]


                              kx ky msq[0, 0, 2]
Mdef[0,0,0]=msq[0, 0, 0] + ------------------
                                     2
                                    c
```

Fig. 8. Program in Mathematica that symbolically computes transformations of moments for the case of superellipsoids.

From (64) and (66) it follows that for half integer arguments $(n = 1, 2, 3, \ldots)$

$$\Gamma(1/2 + n) = \frac{1 \cdot 3 \cdot 5 \ldots (2n-1)}{2^n}\sqrt{\pi}. \tag{67}$$

Below we derive the intermediate result frequently used in computing moments of superellipses and superellipsoids

$$\begin{aligned} B(x, x+1) &= \frac{\Gamma(x)\Gamma(x+1)}{\Gamma(2x+1)} \\ &= \frac{x\Gamma(x)\Gamma(x)}{2x\Gamma(x+1)} \\ &= \frac{1}{2}B(x,x). \end{aligned} \tag{68}$$

Since $\Gamma(x)$ approaches $+\infty$ for $x \to 0^+$ and $-\infty$ for $x \to 0^-$ we have to compute the limits for the beta function terms for the case of rectangular shapes, when $\epsilon \to 0^+$

$$\begin{aligned} \lim_{\epsilon\to 0^+} \epsilon B(a\epsilon, b\epsilon) &= \lim_{\epsilon\to 0^+} \epsilon \frac{\Gamma(a\epsilon)\Gamma(b\epsilon)}{\Gamma((a+b)\epsilon)} \\ &= \lim_{\epsilon\to 0^+} \epsilon \frac{\frac{\Gamma(a\epsilon+1)}{a\epsilon}\frac{\Gamma(b\epsilon+1)}{b\epsilon}}{\frac{\Gamma((a+b)\epsilon+1)}{(a+b)\epsilon}} \\ &= \left(\frac{1}{a}+\frac{1}{b}\right)\lim_{\epsilon\to 0^+}\frac{\Gamma(a\epsilon+1)\Gamma(b\epsilon+1)}{\Gamma((a+b)\epsilon+1)} \\ &= \frac{1}{a}+\frac{1}{b} \end{aligned} \tag{69}$$

and

$$\begin{aligned} \lim_{\epsilon\to 0^+} \epsilon B(a\epsilon, b\epsilon+1) &= \lim_{\epsilon\to 0^+} \epsilon \frac{\frac{\Gamma(a\epsilon+1)}{a\epsilon}\Gamma(b\epsilon+1)}{\Gamma((a+b)\epsilon+1)} \\ &= \frac{1}{a}\lim_{\epsilon\to 0^+}\frac{\Gamma(a\epsilon+1)\Gamma(b\epsilon+1)}{\Gamma((a+b)\epsilon+1)} \\ &= \frac{1}{a}. \end{aligned} \tag{70}$$

## Appendix II
## Computing Transformations of Moments With Mathematica

For the case of transformation where the $f_x, f_y, f_z$ are *polynomials* with multiple variables $x, y, z$ and the $p, q, r$ of $M_{pqr}$ are fixed, the transformation of moments can be computed symbolically with a program in Mathematica presented in Fig. 8. If the object transformed is *not* a superellipsoid, the section between the comment lines $(* *)$ should be removed.

## References


[1] R. J. Prokop and A. P. Reeves, "A survey of moment-based techniques for unoccluded object representation and recognition," *Comput. Vis., Graph., Image Process.*, vol. 54, no. 5, pp. 438–460, 1992.

[2] F. A. Sadjadi and E. L. Hall, "Three-dimensional moment invariants," *IEEE Trans. Pattern Recognit. Machine Intell.*, vol. PAMI-2, pp. 127–136, Mar. 1980.

[3] C. Lo and H. Don, "3-D moment forms: Their construction and application to object identification and positioning," *IEEE Trans. Pattern Recognit. Machine Intell.*, vol. 11, pp. 1053–1064, Oct. 1989.

[4] A. G. Mamistvalov, "$n$-dimensional moment invariants and conceptual mathematical theory of recognition $n$-dimensional solids," *IEEE Trans. Pattern Recognit. Machine Intell.*, vol. 20, pp. 819–831, Aug. 1998.

[5] J. M. Galvez and M. Canton, "Normalization and shape recognition of three-dimensional objects by 3-D moments," *Pattern Recognit.*, vol. 26, no. 5, pp. 667–681, 1993.

[6] A. Jaklič, A. Leonardis, and F. Solina, *Segmentation and Recovery of Superquadrics*, ser. Computational imaging and vision. Norwell, MA: Kluwer, 2000, vol. 20.

[7] M. Y. Zarrugh, "Display and inertia parameters of superellipsoids as generalized constructive solid geometry primitives," in *Proc. 1985 ASME Int. Computers Engineering Conf. Exhibition*, vol. 1, 1985, pp. 317–328.

[8] F. Solina and R. Bajcsy, "Recovery of parametric models from range images: The case for superquadrics with global deformations," *IEEE Trans. Pattern Anal. Machine Intell.*, vol. 12, pp. 131–147, 1990.

[9] P. Whaite and F. P. Ferrie, "From uncertainty to visual exploration," *IEEE Trans. Pattern Anal. Machine Intell.*, vol. 13, pp. 1038–1049, Oct. 1991.

[10] P. J. Besl and N. D. McKay, "A method for registration of 3-D shapes," *IEEE Trans. Pattern Anal. Machine Intell.*, vol. 14, pp. 239–256, Feb. 1992.

[11] G. Turk and M. Levoy, "Zippered polygon meshes from range images," in *Proc. Computer Graphics, Ann. Conf. Series*, 1994, pp. 311–247.

[12] G. Blais and M. D. Levine, "Registering multiview range data to create 3-D computer objects," *IEEE Trans. Pattern Anal. Machine Intell.*, vol. 17, pp. 820–824, 1995.

[13] C. Dorai, J. Weng, and A. K. Jain, "Optimal registration of object views using range data," *IEEE Trans. Pattern Anal. Machine Intell.*, vol. 19, pp. 1131–1138, 1997.

[14] A. H. Barr, "Superquadrics and angle-preserving transformations," *IEEE Comput. Graph. Appl.*, vol. 1, pp. 11–23, Jan. 1981.

[15] F. Solina, "Shape Recovery and Segmentation with Deformable Part Models," Ph.D. dissertation, Univ. Pennsylvania, Philadelphia, PA, 1987.

[16] A. Leonardis, A. Jaklič, and F. Solina, "Superquadrics for segmentation and modeling range data," *IEEE Trans. Pattern Recognit. Machine Intell.*, vol. 19, pp. 1289–1295, Nov. 1997.

[17] K. Arun, T. Huang, and S. Blostein, "Least-squares fitting of two 3-D point sets," *IEEE Trans. Pattern Recognit. Machine Intell.*, vol. 9, pp. 698–700, Sept. 1987.

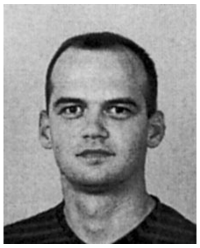

**Aleš Jaklič** (M'97) received the B.S. and M.S. degrees in electrical engineering and the Ph.D. degree in computer science from the University of Ljubljana, Ljubljana, Slovenia in 1989, 1992, and 1997, respectively.

He is currently Teaching Assistant at the Faculty of Computer and Information Science, University of Ljubljana. During visits to the University of Pennsylvania, Philadelphia, in 1990, 1992, 1995, and 1998 he worked as a Research Assistant at the GRASP Laboratory and was a post-doctoral Partridge Fellow in 1997 at Fitzwilliam College, University of Cambridge, Cambridge, U.K. His research interests include range image interpretation, 3-D shape reconstruction, multimedia, and internet technologies.

**Franc Solina** (SM'98) received the B.S. and M.S. degrees in electrical engineering from the University of Ljubljana, Ljubjana, Slovenia in 1979 and 1982, respectively, and the Ph.D. degree in computer science from the University of Pennsylvania, Philadelphia, in 1987.

He is a Professor of computer science at the University of Ljubljana, Ljubljana, Slovenia and Head of Computer Vision Laboratory at the Faculty of Computer and Information Science. His research interests include range image interpretation, 3-D shape reconstruction, panoramic imaging, and applications of computer vision in the arts.